ELSEVIER

J. Non-Newtonian Fluid Mech. 137 (2006) 103–109

Journal of Non-Newtonian Fluid Mechanics

www.elsevier.com/locate/jnnfm

Charge screening effects on filament dynamics in xanthan gum solutions

Linda B. Smolka*, Andrew Belmonte

The W.G. Pritchard Laboratories, Department of Mathematics, Pennsylvania State University, University Park, PA 16802, USA

Received 2 June 2005; accepted 31 January 2006

Abstract

We experimentally investigate the filament dynamics of non-Newtonian drops falling under gravity through air, and report the effects of semi-dilute concentrations of the polyelectrolyte polymer xanthan gum mixed in 80:20 glycerol/water with varying concentrations of potassium chloride (KCl). We find that the addition of 780 ppm xanthan gum to the glycerol/water solvent dramatically increases the drop length just before pinch-off, by two orders of magnitude. This length is decreased by as much as an order of magnitude with the addition of KCl. The qualitative dynamics of bead formation on the filament is also very sensitive to added salt. These experimental observations are related to well-known changes in the molecular structure of xanthan gum due to charge screening effects.

Keywords: Liquid drops; Liquid filament; Extensional flow; Drop length; Bead-on-string; Xanthan gum; Polyelectrolyte polymer; Charge screening

1. Introduction

The formation of Newtonian fluid drops in air has long been an active area of research fueled by theoretical and experimental studies, numerical simulations, and industrial applications. The earliest related studies date back to the work of Plateau [1] and Rayleigh [2]. More recent studies of droplet formation and pinch-off include experimental [3–6], theoretical [3,4,7,8], and numerical studies [3,6] (for a thorough review of the subject see [9]). One striking aspect of this process is the long fluid filament drawn out by the falling drop while still attached to the orifice. When the fluid contains macromolecules (such as polymers), or is otherwise non-Newtonian [10,11], these filaments can become extraordinarily long and long-lived. Moreover, many new phenomena are observed, such as filament stabilization, (elastic) retraction, and the development of bead-on-string perturbations along the filament [10,12–14].

In the Newtonian case it is well known that the magnitude of the viscosity plays an important role in the formation of falling drops, in particular for the maximum length attained by the filament before pinch-off and the stability of the filament to perturbations [3–5]; the filament can be relatively short at low viscosities (e.g., water) and longer at higher viscosities (e.g., corn syrup). As the flow field in an axisymmetric filament is almost purely extensional, the relevant quantity is extensional viscosity $\hat{\eta}$, which is the proportionality constant between the normal stress difference and the stretch rate $\dot{\epsilon}$ [15]. For a Newtonian fluid $\hat{\eta}$ is simply related to the shear viscosity η: the Trouton ratio $\hat{\eta}/\eta$ is constant and equal to 3 [15,16]. For a non-Newtonian fluid, it is not entirely clear, which property is the cause of the stabilization. The fact that the Trouton ratio may exceed 3, and values up to ∼1000 are observed [17], may be responsible for some or all of these effects. However, the elastic and normal stress effects may also play a role.

Among aqueous polymer solutions, polyelectrolytes derive many of their important properties from the fact that their molecular conformational state is sensitive to the ionic environment; proteins and DNA are particular examples. A polyelectrolyte polymer typically swells when placed in a low ionic strength solution due to electrostatic self-repulsion [18]. The work presented here examines the dynamics of falling drops using a solution of the polyelectrolyte polymer xanthan gum [19]. The molecular and resultant rheological properties of this polymer are known to be modified by the addition of salt. Our study shows that the hydrodynamic flow of xanthan gum solutions in filaments is surprisingly sensitive to the added salt concentration. This sensitivity provides an excellent example of the coupling between molecular and macroscopic fluid dynamics which is possible in complex fluids.

* Corresponding author at: Department of Mathematics, Bucknell University, Lewisburg, PA 17837, USA. Tel.: +1 570 577 3563; fax: +1 570 577 3264.
E-mail address: lsmolka@bucknell.edu (L.B. Smolka).

0377-0257/$ – see front matter © 2006 Elsevier B.V. All rights reserved.
doi:10.1016/j.jnnfm.2006.01.012

2. Experimental setup and rheology

Our study of non-Newtonian drops was conducted with solutions of xanthan gum, a high molecular weight ($\approx 5 \times 10^6$), water-soluble, anionic polysaccharide produced by the bacterium *Xanthomonas Campestris* [19]. The properties of xanthan gum have made it an appealing product for use in a variety of industries including the food, cosmetic, agricultural, and petroleum industries [19,20], as well as laboratory experiments [21,22]. The xanthan molecule consists of a backbone of four glucose units with charged side-chains located at alternating units [19,20]. As a polyelectrolyte polymer, its molecular structure depends primarily on the ionic strength of the side-chains and the free ions in the solvent [18]. In an aqueous solution with no added ions, the xanthan molecule is extended due to the electrostatic repulsion of the negatively charged side-chains. When salt is added to semi-dilute solutions (about 200–2000 ppm) [23], charge screening causes the side chains to collapse down to the backbone, driving a transition in the structure which gives the xanthan molecule a rigid rod-like shape [20] (and reduces its hydrodynamic size). These molecular changes are known to affect the rheological properties, and one expects the fluid dynamics of these solutions to change as well.

The xanthan gum used in our experiments was a commercially available product (Vanzan NF) provided by R.T. Vanderbilt Co. (Norwalk, CT). We mixed various concentrations of xanthan gum and potassium chloride KCl (Baker) in an 80:20 (by weight) glycerol and distilled de-ionized water solution. The solutions were prepared by first adding water to the xanthan gum and KCl powder and gently mixing until all microgels of the gum appeared dissolved. Since xanthan gum has a high resistance to shear degradation, we were not concerned about the effects of this mixing. Glycerol was then added, and the solution was mixed for up to 24 h, and allowed to sit for another day before use. We have studied two concentrations of xanthan gum (390 and 780 ppm, corresponding to 0.039 and 0.078 wt.%) and a range of salt concentrations ([KCl] = 0–3.125%). The surface tension was measured at room temperature using a Fisher model 21 tensiomat, and varied by 1% from $\gamma = 67.4$ dyn/cm. The fluid density varied by less than 1% from $\rho = 1.28$ g/cm^3. The fluids and their properties used in our study are listed in Table 1.

We measured the steady and transient rheological properties of our xanthan gum solutions in shear as a way to monitor the molecular changes induced by the added salt; the shear rheology is not directly relevant to the essentially extensional flow in the filament. The measurement of extensional rheology is at present much more difficult than shear rheology, due to the geometrical challenges of providing a constant $\dot{\epsilon}$ flow (see e.g., [17,24]). While indirect techniques are available, such as opposed jets [23], we did not make any extensional rheology measurements in this study.

Shear rheology measurements were made with a temperature-controlled cone and plate rheometer (Brookfield, Model DV-III+) in constant shear rate mode, in a range from 15 to 500 s^{-1}, and at 21.9 °C. Fig. 1 shows shear stress as a function of shear rate for several of the fluids used in our study. The stress T_{12} and shear rate $\dot{\gamma}$ data follow a power-law relationship $T_{12} = C(\dot{\gamma})^n$ (as is commonly observed [15]), where n and C are constants; for a Newtonian fluid $n = 1$ and $C = \eta$. Values of n and C are reported in Table 1. We find that all of the 780 ppm xanthan/KCl solutions are shear-thinning ($n < 1$), in agreement with previous studies [19,20,25,26]. Also, over the range of shear rates tested the salt-free xanthan solution had the highest effective shear viscosity $T_{12}/\dot{\gamma}$, which decreased with increasing salt concentration. We note that at the lower xanthan concentration (390 ppm), the high salt solution (3.125%) was nearly Newtonian ($n = 0.97$), while the salt-free solution was significantly non-Newtonian ($n = 0.77$) [27].

Semi-dilute solutions of xanthan gum are known to be elastic [20,28,29]. We characterize this elasticity by measuring the transient residual shear stress. First, a steady flow producing a shear stress of $T_{12} = 100$ dyn/cm^2 was applied for 3000 s in a cone and plate rheometer [27]. The transient stress was recorded for 24 s or more after the shear was turned off, as shown for several cases in Fig. 2(a). The data does not follow a simple relaxation behavior $T_{12} \sim \mathrm{e}^{-t/\lambda}$ [15], so we determined a characteristic relaxation time using the time for the shear stress to decrease to 1% of the applied value. Since Newtonian fluids are inelastic, we used the pure solvent and a commercial vegetable oil as the control for this measurement. It took on average 2.1 s for the shear stress to reach 1 dyn/cm^2 for these two Newtonian fluids, which we assumed to be a mechanical artifact of the rheometer (the xanthan solutions took longer). We define the effective

Table 1
Fluid properties of solutions in 80:20 glycerol and water

Xanthan gum (% conc.)	KCl (% conc.)	γ (dyn/cm)	ρ (g/cm^3)	η index, n	η prefactor, C	Effective relaxation time, t_r (s)
0	0	66.2	1.28	0.98	0.895	0
0.039	0	68.1	1.27	0.77	4.13	6.9
0.039	3.125	67.3	1.28	0.97	0.83	0.7
0.078	0	68.3	1.27	0.73	7.51	23.8
0.078	0.013	67.7	1.27	0.79	4.75	13.8
0.078	0.024	67.0	1.28	0.76	4.65	9.9
0.078	0.035	66.9	1.27	0.75	4.97	–
0.078	0.047	67.4	1.27	0.78	4.45	8.8
0.078	0.117	68.2	1.28	0.79	4.03	7.3
0.078	0.391	66.6	1.28	0.79	3.95	5.3
0.078	1.563	67.8	1.29	0.85	3.09	3.5
0.078	3.125	67.5	1.27	0.80	3.23	2.9

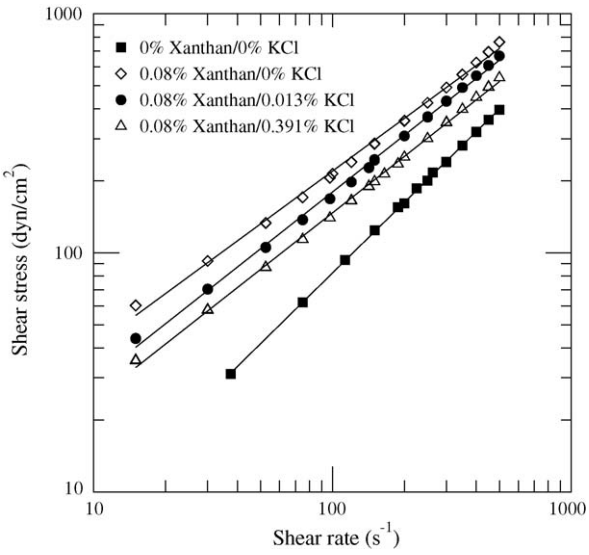

Fig. 1. Shear stress T_{12} (dyn/cm^2) vs. shear rate $\dot{\gamma}$ (s^{-1}) for several fluids. The straight lines represent fits of the data for each fluid to $T_{12} = C(\dot{\gamma})^n$, with C and n for all 12 fluids listed in Table 1.

relaxation time t_r for each fluid as the difference between the measured time and 2.1 s; values of t_r are reported in Table 1.

The long decay for the shear stress in the 780 ppm xanthan gum solution with no salt ($t_r = 23.8$ s) indicates that this solution is highly elastic; at lower xanthan concentration (390 ppm), the fluid is less elastic ($t_r = 6.9$ s). The elasticity also decreases with increasing salt levels. Fig. 2(b) is a plot of the effective relaxation time as a function of [KCl] for the 780 ppm xanthan gum solutions. A least squares fit of the data, represented by the solid line, indicate that $t_r \sim [\mathrm{KCl}]^{-0.30}$. This scaling is in disagreement with the Rouse model for polyelectrolyte solutions [30], which for the xanthan gum used in our experiments has the form

$$t_r \sim \left[1 + \frac{2[\mathrm{KCl}]}{3[\mathrm{XG}]}\right]^{-3/4},$$

where [XG] denotes the concentration of xanthan gum. The scaling $t_r \sim [\mathrm{KCl}]^{-3/4}$ occurs in the high salt concentration limit where there are many more salt ions than free counterions (i.e. $[\mathrm{KCl}] \gg 1.5\,[\mathrm{XG}]$). The xanthan gum solutions shown in Fig. 2(b) are in this limit, with the relevant ratio $3 \times 10^3 \leq 2[\mathrm{KCl}]/3[\mathrm{XG}] \leq 7 \times 10^5$. The effective shear viscosity ($T_{12}/\dot{\gamma}$) of polyelectrolyte solutions scales in the same way as the relaxation time, and it has been verified experimentally that the viscosity of flexible polyelectrolyte solutions (sulfonated polystyrene [31] and polyacrylic acid [32]) follow a $-3/4$ scaling. If xanthan gum is sufficiently rigid then its conformation may not change as much with the addition of salt, and this may account for the weaker dependence of the relaxation time on salt concentration that we observe [33]. Finally, we note that at the lower xanthan concentration 390 ppm, the addition of 3.125% salt makes the fluid essentially inelastic ($t_r = 0.7$ s).

The experimental apparatus that produced the drops was similar to those used previously [4]. The fluid flow was driven by gravity from a 32 cm^3 plastic (Lucite) reservoir, which was open to the atmosphere, into a tube of length 2.5 cm, through a needle valve, which controlled the flow rate, and finally through a lower tube of length 6.6 cm with inner and outer radii of 1.54 and 2.17 mm. The 0.63-mm-wide edge of the orifice was machined flat to allow for a reproducible contact line at the orifice/fluid/air interface. In all of the experiments the period of the drops was about 30 s/drop. The experimental apparatus was set on a vibration isolated table and enclosed in a box to reduce air currents. Images and video sequences of the drops were obtained using a Kodak Ektapro 1012 EM Motion Analyzer; details of the illumination used in these experiments can be found in [4]. The spatial resolution of the images ranged between 0.14 and 0.64 mm/pixel. The temporal resolution in the experiments ranged between 3000–4000 images/s.

For very long drops (exceeding 15 cm in length) we were unable to image the whole drop from the orifice to the drop tip at the time of pinch-off. In this case, the length was measured over several camera positions, during which the period of the

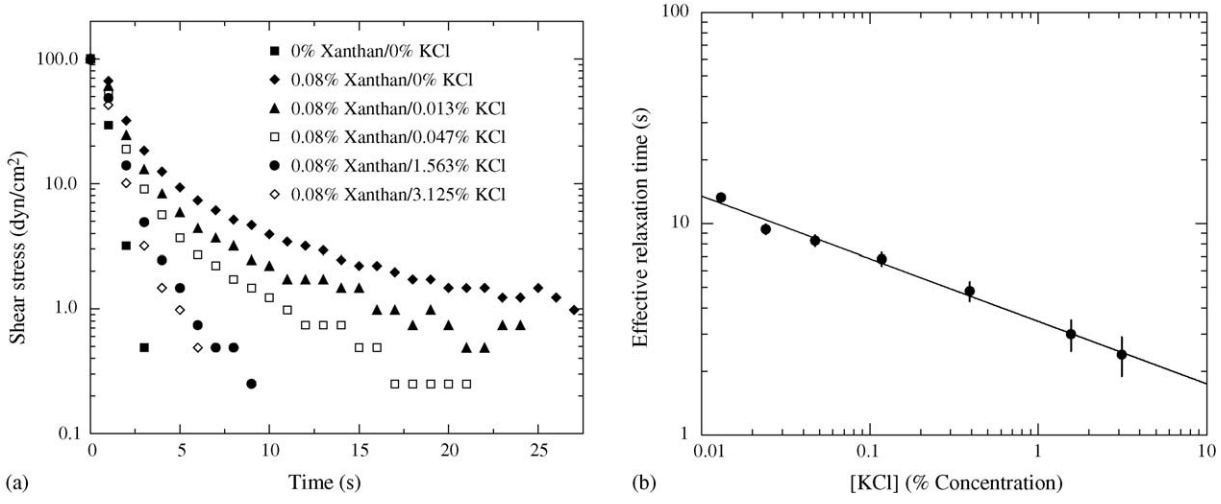

Fig. 2. (a) Transient shear stress (dyn/cm^2) vs. time (s). (b) Effective relaxation time t_r (s) vs. [KCl] for solutions of 780 ppm xanthan gum. The solid line is a least squares fit to $t_r = 3.45\,[\mathrm{KCl}]^{-0.30}$.

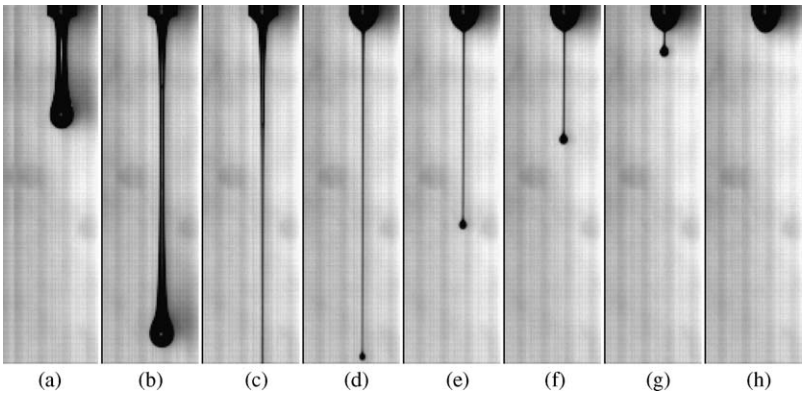

Fig. 3. Evolution of a drop of 390 ppm xanthan gum in 80:20 glycerol/water with no salt. The size of each image is 1.45 cm × 5.41 cm. The relative times of each image are (a) 0 ms, (b) 325 ms, (c) 444 ms, (d) 599 ms, (e) 619 ms, (f) 633 ms, (g) 649 ms, and (h) 666 ms.

drops and fluid temperature were held constant (within 6%). We moved the camera down vertically at 5 cm increments until we observed the pinch-off of the filament before the falling drop exited the screen.

3. Filament stability and pinch-off length

The initial formation of a drop of xanthan gum solution falling through air produces a thin filament connected to the orifice, similar to a Newtonian fluid. The filament is dependent on several non-dimensional parameters, which characterize the fluid dynamics near the orifice.

For all experiments here the period of the drops is held fixed at approximately 30 s/drop, or a volume flow rate of $5.1 \times 10^{-4}\,\mathrm{cm}^3/\mathrm{s}$ (assuming a drop volume of $4\pi R^3/3$, and using the orifice radius $R = 0.154\,\mathrm{cm}$). Thus we estimate the average velocity at the orifice to be $U_0 \simeq 6.8 \times 10^{-3}\,\mathrm{cm/s}$, which for the 80:20 glycerol/water solvent gives a Reynolds number of $Re = \rho U_0 R/\eta = 2 \times 10^{-3}$; the Bond number is $Bo = \rho g R^2/\gamma = 0.45$. From these two parameters, we conclude that the initial droplet formation is viscous, and characterized by a balance in the gravitational and capillary forces which allows pendant drops to form. Since the surface tension and density of the fluids vary by less than 1% and the flow rate was held fixed, we expect the drop volume to be nearly constant in all of the experiments.

Using the most elastic fluid, we estimate the maximum Deborah number of the flow near the orifice to be $De = t_r U_0/R \simeq 1$. However, because a drop falls only every 30 s, we expect that the polymers are initially relaxed. Once the drop begins to fall away from the orifice it draws out a long, fluid filament (see Fig. 3(a) and (b)). A comparison of the interfacial motion of this filament for the 780 ppm xanthan gum solution with $0\% \leq [\mathrm{KCl}] \leq 0.047\%$ to an analytic model shows strong quantitative agreement [34]. The model, which also provides the stretch rate in the filament, predicts $De > 1$ over a transient period while the filament initially stretches [34]. After this transient period, the stretch rate monotonically decreases so that eventually $De < 1$ [34]. Thus we expect viscoelastic effects to be relevant to the filament motion during some initial time period in the experiment.

The dynamics of filament formation and drop pinch-off are shown in Figs. 3 and 4 for two different salt concentrations. The fluid shown in Fig. 3 is the 390 ppm xanthan gum/80:20 glyc-

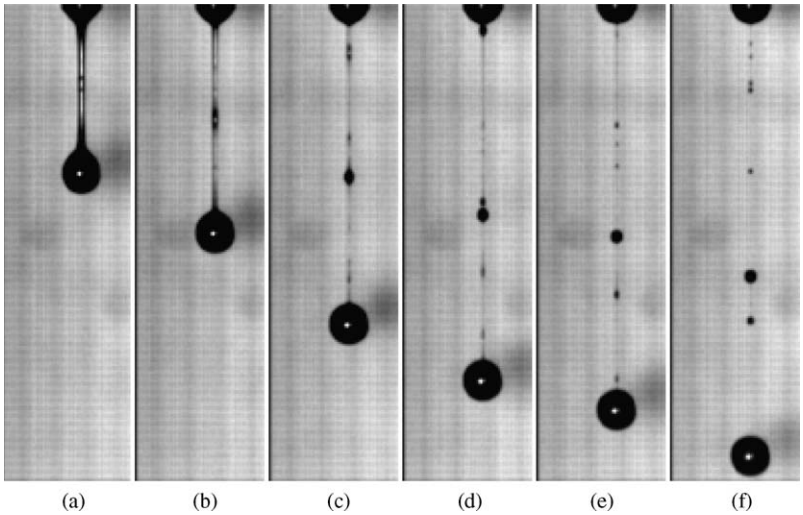

Fig. 4. Evolution of a drop of 390 ppm xanthan gum and 3.125% KCl mixed in 80:20 glycerol/water. The size of each image is 1.45 cm × 5.41 cm. The relative times of each image are (a) 0 ms, (b) 15.7 ms, (c) 33.3 ms, (d) 42.3 ms, (e) 46.7 ms, (f) 53 ms.

erol/water solution with no salt. In Fig. 3(a) the drop is falling away from the orifice. As the filament lengthens, its diameter appears to taper toward its center in the axial direction (frames (b) and (c)). The drop pinches off between frames (c) and (d), out of the camera's view. Since the filament does not pinch-off at its connection to the orifice, the type of pinch-off can be characterized as internal-pinching [4]. Remarkably, a large portion of the filament (at least 5 cm in length) retracts back into the orifice, in frames (d) through (h). During this time the filament appears to be free of perturbations and uniform in diameter. The small spherical drop at the tip of the retracting filament suggests this flow is elastically driven, rather than the surface tension driven retraction common in Newtonian fluids [9].

By contrast, Fig. 4 shows the dynamics of a mixture of 80:20 glycerol/water with 390 ppm xanthan gum and 3.125% KCl. Comparing the sequence of images in Figs. 3 and 4 we see the dramatic changes in the drop dynamics due to the addition of salt. As the drop falls away from the orifice a perturbation along the filament interface is already apparent in Fig. 4(a). In the images that follow, this perturbation grows in size, while other perturbations of varying size develop along the filament interface. This well-known bead-on-string instability does not immediately cause the filament to break [10,12,13]. Several of these perturbations retract into either the orifice, the largest perturbation, or the drop. For example, the perturbation at the top of the filament in frame (c) has traveled upward by frame (d), and by frame (e) it has retracted into the fluid at the orifice. The filament internally pinches off between frames (e) and (f), causing several satellite drops to form.

The most dramatic effect of the xanthan polymer (with and without salt) on the filament appears in the length of the drop at the moment of pinch-off. The pinch-off length of the drop L_p is defined to be the distance from the orifice to the drop tip at the time of pinch-off (also called the drop length). For the drop in Fig. 4, $L_p \simeq 4.8$ cm. In Fig. 5 this length is shown as a function of salt concentration [KCl] for the 780 ppm xanthan solution; (●) represents the average value of L_p and the resolution bars indicate the range of L_p observed in the experiments. The dashed line in the figure is the drop length of the 80:20 glycerol/water solvent only: $L_p = 1.4$ cm, reproducible to within 1%. The addition of xanthan gum to this Newtonian solvent has a significant effect on the drop length. For the salt-free 780 ppm xanthan gum solution, the drop length varies from 80 cm to over 1 m. Thus a very small amount of xanthan gum produces an increase in the pinch-off length by a factor of 60–70 over the Newtonian drop.

The addition of salt to the 780 ppm xanthan gum solution produces a striking change in the dynamics of the drop during pinch-off, which depends strongly on salt concentration. At very low values ([KCl] $\leq 0.013\%$), the drop length is not much different from the pure xanthan gum/glycerol/water solution. However for larger salt concentrations, [KCl] $\geq 0.035\%$ the drop lengths decrease to an average value of 11 cm. At these higher concentrations we found L_p varied by as much as 16% from drop to drop for the same fluid (and the same approximate temperature and flow rate). Based on the data in Fig. 5, we define a critical salt concentration $[KCl]_c \approx 0.02\%$, around which the drop

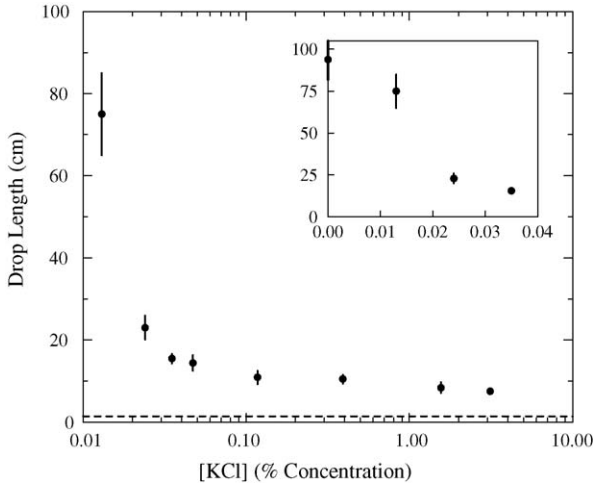

Fig. 5. Pinch-off length L_p vs. [KCl] for 780 ppm xanthan gum in 80:20 glycerol/water. The symbol (●) represents the average value of L_p over all experiments, and the resolution bars indicate the range of L_p observed. The value of L_p for the solvent is denoted by the dashed line. The inset is a linear plot of L_p vs. [KCl] at low salt concentrations.

length changes by over a factor of 3. Note that the drop length is fairly insensitive to salt concentrations above $[KCl]_c$.

For the lower concentration xanthan gum solution (390 ppm) with no salt, we also found that the drop is significantly longer than the Newtonian solvent with values ranging from 75 cm to over 1 m. At a high salt concentration (3.125%) the drop length decreased to an average value of 6.3 cm. We were interested to see if the drop length could be further decreased to that of the Newtonian solvent for an even higher salt concentration. However for [KCl] $> 3.125\%$ the solution was saturated with salt, so this hypothesis could not be verified.

4. Discussion

Two striking aspects of our observations of the filament produced by a falling drop of xanthan gum solution are evident in Fig. 5: the dramatic increase in the drop length of the polymer solution relative to the Newtonian solvent, and the sensitivity of this length to salt concentration. These results can be explained by considering previous studies that address: (i) the influence of xanthan gum in extensional flows, and (ii) the dependence of the molecular structure on salt concentration.

We find the drop length is strongly dependent on salt concentration around a critical value of $[KCl]_c$. In measurements of the shear viscosity of an aqueous xanthan solution, Rochefort and Middleman observed that at a critical salt concentration, the molecular structure of xanthan gum transitions from a disordered to an ordered state; once in this ordered state the molecules are relatively insensitive to further increases in salt level [20]. They estimate the transition occurs at $[NaCl]_c \approx 10^{-3}$ M for a 250 ppm xanthan gum solution. The jump in drop length that we observe for a 780 ppm xanthan gum solution occurs at $[KCl]_c \approx 0.02\%$ or 3×10^{-3} M. We attribute our observed transition in drop length as due to the disorder/order transition described by Rochefort and Middleman. This hypothesis is further supported by the fact that the drop length was fairly

insensitive to salt levels above $[KCl]_c$. Note that our polymer concentration is three times larger than their case, consistent with the rough factor of 3 in our $[KCl]_c$ over their transition concentration.

How do the hydrodynamics of the polymer couple to the filament dynamics? As previously stated, the extensional viscosity is the relevant quantity in the flow field of the filament. By referring to previous studies, we estimate the extensional viscosity of our solutions with no salt. These estimates appear sufficient to account for the enormous increase in the drop length. While our solutions are also very elastic, the variation in elasticity with salt concentration (Fig. 2) does not appear adequate to explain the increase in drop length.

In an experimental study with dilute xanthan gum mixtures (no salt), Fuller et al. [35] found that a steady state extensional viscosity was attained at very low stretch rates. For 100 ppm xanthan gum in 80:20 glycerol/water, they report $\hat{\eta} \approx 35$ P. In another experimental study, Khagram et al. [36] measured the extensional viscosity of 500 ppm xanthan gum in 75:25 glycerol/water, and also found that $\hat{\eta}$ tends to an $\dot{\epsilon}$ independent limit (about 400 P) for times greater than the reciprocal of a characteristic stretch rate. Since xanthan is a rigid molecule it does not stretch out in an extensional flow; it is the alignment of the molecules along the flow that cause the extensional viscosity to reach a steady state at low stretch rates [29]. Based on the results of [35,36], we expect the extensional viscosity of our 780 ppm xanthan solution to be larger than 400 P. Since $\hat{\eta} \simeq 2.4$ P for our Newtonian solvent [37], this would represent an increase of two orders of magnitude, the same order as the drop length increase (from 1.4 cm to 1 m). This would be consistent with the pinch-off length being proportional to the extensional viscosity; to confirm such a relationship, an independent measurement of $\hat{\eta}$ versus [KCl] is obviously required. Our hypothesis is partially supported by measurements made by Carrington et al. [23] who found the extensional viscosity of dilute xanthan solutions decrease with the addition of salt, although their experiments were at lower xanthan concentrations. As far as the present study, we have not yet found the direct rheological connection between the concentration of added salt and the enormous changes observed in L_p and the drop dynamics.

5. Conclusion

We have presented measurements of the drop length before pinch-off in a xanthan gum solution as a function of KCl concentration. These results demonstrate the macroscopic consequences of charge screening in extensional flows of polyelectrolytes, specifically showing that xanthan gum solutions provide a useful experimental fluid in which the elasticity and other non-Newtonian aspects can be easily varied, while other properties (surface tension, density) remain fixed. The addition of salt affects the elasticity, shear viscosity, and also drop length at pinch-off. This last effect is strikingly sensitive: the drop length increases by $\sim$50 cm when the salt concentration is decreased by $\sim$0.01%. This change coincides with a previously reported molecular transition in xanthan gum driven by charge screening effects. The apparent connection between drop length and extensional viscosity (or Trouton ratio) is worthy of further investigation which we leave for a future study.

Acknowledgments

We would like to thank R.H. Colby, D.M. Henderson, A. Jayaraman, M.J. Shelley, P. Palffy-Muhoray, M. Rubinstein, and D. Bonn for discussions and suggestions, and R. Geist, A. Young and J. Marden for help with aspects of the experiments. AB acknowledges support from the A.P. Sloan Foundation and the National Science Foundation (CAREER Award DMR-0094167). LBS acknowledges partial support from the National Science Foundation (VIGRE grant DMS-9983320).

References

[1] J. Plateau, Statique experimentale et theorique des liquides soumis aux seules forces moleculaires, vol. II, Gauthier-Villars, Paris, 1873, p. 319.
[2] W.S. Rayleigh, On the instability of jets, Proc. Lond. Math. Soc. 10 (1878) 4–13.
[3] X.D. Shi, M.P. Brenner, S.R. Nagel, A cascade of structure in a drop falling from a faucet, Science 265 (1994) 219–222.
[4] D.M. Henderson, H. Segur, L.B. Smolka, M. Wadati, The motion of a falling liquid filament, Phys. Fluids 13 (2000) 550–565.
[5] X. Zhang, O.A. Basaran, An experimental study of the dynamics of drop formation, Phys. Fluids 7 (1995) 1184–1203.
[6] E.D. Wilkes, S.D. Phillips, O.A. Basaran, Computational and experimental analysis of dynamics of drop formation, Phys. Fluids 11 (1999) 3577–3598.
[7] J. Eggers, Theory of drop formation, Phys. Fluids 7 (1995) 941–953.
[8] S.E. Bechtel, C.D. Carlson, M.G. Forest, Recovery of the Rayleigh capillary instability from slender 1-D inviscid and viscous models, Phys. Fluids 7 (1995) 2956–2971.
[9] J. Eggers, Nonlinear dynamics and breakup of free-surface flows, Rev. Modern Phys. 69 (1997) 865–930.
[10] M. Goldin, J. Yerushalmi, R. Pfeffer, R. Shinnar, Breakup of a laminar capillary jet of a viscoelastic fluid, J. Fluid Mech. 38 (1969) 689–711.
[11] R.P. Mun, J.A. Byars, D.V. Boger, The effects of polymer concentration and molecular weight on the breakup of laminar capillary jets, J. Non-Newtonian Fluid Mech. 74 (1998) 285–297.
[12] M.S.N. Oliveira, G.H. McKinley, Iterated stretching and multiple beads-on-a-string phenomena in dilute solutions of highly extensible flexible polymers, Phys. Fluids 17 (2005) 071704.
[13] M.C. Sostarecz, A. Belmonte, Beads-on-string phenomena in wormlike micellar fluids, Phys. Fluids 16 (2004) L67–L70.
[14] M. Renardy, Some comments on the surface tension driven break-up (or the lack of it) of viscoelastic jets, J. Non-Newtonian Fluid Mech. 51 (1994) 97–107.
[15] R.B. Bird, R.C. Armstrong, O. Hassager, Dynamics of Polymeric Liquids, vol. 1, 2nd ed., Wiley and Sons, New York, 1987.
[16] F.T. Trouton, On the coefficient of viscous traction and its relation to that of viscosity, Proc. Roy. Soc., London A77 (1906) 426–440.
[17] T. Sridhar, V. Tirtaatmadja, D.A. Nguyen, R.K. Gupta, Measurement of extensional viscosity of polymer solutions, J. Non-Newtonian Fluid Mech. 40 (1991) 271–280.
[18] F. Oosawa, Polyelectrolytes, 2nd ed., M. Dekker, New York, 1971.
[19] A. Nussinovitch, Hydrocolloid Applications, Blackie Academic & Professional, New York, 1997.
[20] W.E. Rochefort, S. Middleman, Rheology of xanthan gum: salt, temperature, and strain effects in oscillatory and steady shear experiments, J. Rheol. 31 (1987) 337–369.
[21] D. Bonn, J. Meunier, Viscoelastic free-boundary problems: non-Newtonian viscosity vs. normal stress effects, Phys. Rev. Lett. 79 (1997) 2662–2665.
[22] A. Lindner, D. Bonn, J. Meunier, Viscous fingering in a shear-thinning fluid, Phys. Fluids 12 (2000) 256–261.

[23] S. Carrington, J. Odell, L. Fisher, J. Mitchell, L. Hartley, Polyelectrolyte behaviour of dilute xanthan solutions: salt effects on extensional rheology, Polymer 37 (1996) 2871–2875.
[24] G.H. McKinley, A decade of filament stretching rheometry, in: D.M. Binding, N.E. Hudson, J. Mewis, J.-M. Piau, C.J.S. Petrie, P. Townsend, M.H. Wagner, K. Walters (Eds.), Proceedings of the XIIIth International Congress Rheology, vol. 1, British Society of Rheology, Cambridge, UK, 2000, pp. 15–22.
[25] P.J. Whitcomb, C.W. Macosko, Rheology of Xanthan Gum, J. Rheol. 22 (1978) 493–505.
[26] M. Milas, M. Rinaudo, M. Knipper, J.L. Schuppiser, Flow and viscoelastic properties of xanthan gum solutions, Macromolecules 23 (1990) 2506–2511.
[27] L.B. Smolka, On the Motion of Newtonian and non-Newtonian Liquid Filaments: Stretching, Beading, Blistering, Pinching, PhD Thesis, Pennsylvania State University, 2002.
[28] G.B. Thurston, G.A. Pope, Shear rate dependence of the viscoelasticity of polymer solutions. II. Xanthan gum, J. Non-Newtonian Fluid Mech. 9 (1981) 69–78.
[29] M.A. Zirnsak, D.V. Boger, V. Tirtaatmadja, Steady shear and dynamic rheological properties of xanthan gum solutions in viscous solvents, J. Rheol. 43 (1999) 627–650.
[30] A.V. Dobrynin, R.H. Colby, M. Rubinstein, Scaling theory of polyelectrolyte solutions, Macromolecules 28 (1995) 1859–1871.
[31] D.C. Boris, R.H. Colby, Rheology of sulfonated polystyrene solutions, Macromolecules 31 (1998) 5746–5755.
[32] A.J. Konop, R.H. Colby, Polyelectrolyte charge effects on solution viscosity of poly(acrylic acid), Macromolecules 32 (1999) 2803–2805.
[33] R.H. Colby, private communication.
[34] L.B. Smolka, A. Belmonte, D.M. Henderson, T.P. Witelski, Exact solution for the extensional flow of a viscoelastic filament, Eur. J. Appl. Math. 15 (2004) 679–712.
[35] G.G. Fuller, C.A. Cathey, B. Hubbard, B.E. Zebrowski, Extensional viscosity measurements for low-viscosity fluids, J. Rheol. 31 (1987) 235–249.
[36] M. Khagram, R.K. Gupta, T. Sridhar, Extensional flow of xanthan gum solutions, J. Rheol. 29 (1985) 191–207.
[37] R.C. Weast, M.J. Astle, CRC Handbook of Chemistry and Physics, 63rd ed., CRC Press, Boca Raton, 1982.